FOCUSED COLLECTION

Temperature Effects on DNA Damage during Hibernation*

Lauren de Wit[1,†]
Maarten R. Hamberg[1]
Anne M. Ross[1]
Maaike Goris[2]
Fia F. Lie[2]
Thomas Ruf[3]
Sylvain Giroud[3]
Robert H. Henning[2]
Roelof A. Hut[1]
[1]Groningen Institute for Evolutionary Life Sciences, Chronobiology Unit, University of Groningen, Groningen, The Netherlands; [2]Department of Clinical Pharmacy and Pharmacology, University of Groningen, University Medical Center Groningen, Groningen, The Netherlands; [3]Research Institute of Wildlife Ecology, Department of Interdisciplinary Life Sciences, University of Veterinary Medicine Vienna, Vienna, Austria

Accepted 9/23/2022; Electronically Published 1/27/2023

Online enhancement: appendix.

ABSTRACT

During multiday torpor, deep-hibernating mammals maintain a hypometabolic state where heart rate and ventilation are reduced to 2%–4% of euthermic rates. It is hypothesized that this ischemia-like condition may cause DNA damage through reactive oxygen species production. The reason for intermittent rewarming (arousal) during hibernation might be to repair the accumulated DNA damage. Because increasing ambient temperatures (T_a's) shortens torpor bout duration, we hypothesize that hibernating at higher T_a's will result in a faster accumulation of genomic DNA damage. To test this, we kept 39 male and female garden dormice at a T_a of either 5°C or 10°C and obtained tissue at 1, 4, and 8 d in torpor to assess DNA damage and recruitment of DNA repair markers in splenocytes. DNA damage in splenocytes measured by comet assay was significantly higher in almost all torpor groups than in summer euthermic groups. Damage accumulates in the first days of torpor at $T_a = 5$°C (between days 1 and 4) but not at $T_a = 10$°C. At the higher T_a, DNA damage is high at 24 h in torpor, indicating either a faster buildup of DNA damage at higher T_a's or an incomplete repair during arousals in dormice. At 5°C, recruitment of the DNA repair protein 53BP1 paralleled the increase in DNA damage over time during torpor. In contrast, after 1 d in torpor at 10°C, DNA damage levels were high, but 53BP1 was not recruited to the nuclear DNA yet. The data suggest a potential mismatch in the DNA damage/repair dynamics during torpor at higher T_a's.

Keywords: hibernation, torpor, DNA damage, DNA strand breaks, *Eliomys quercinus*, DNA repair.

Introduction

Hibernation is an energy-conserving strategy in small-bodied hibernators, which typically alternate between periods of low metabolism (torpor) and shorter periods of euthermia (arousals). Hibernation thus conserves energy and increases longevity when compared with animals that remain euthermic (Lyman et al. 1981; Turbill et al. 2011). The lengths of torpor bouts vary during the hibernation season, typically lengthening during the beginning and middle of hibernation and shortening again during the last weeks of hibernation. In addition, ambient temperature (T_a) has a strong effect on torpor bout duration, with the longest torpor bouts observed at T_a's around 4°C (Lyman 1948; Pajunen 1983; Buck and Barnes 2000). Between T_a's of 0°C and 16°C, torpor metabolic rate can increase, but it remains at low absolute levels, resulting in core body temperatures (T_b's) stably regulated within ~1°C above ambient in this temperature range (Pajunen 1992; Buck and Barnes 2000; Hut et al. 2002*a*; Geiser and Kenagy 2016).

Arousing from torpor is the most energetically demanding period during hibernation, which underlines the importance of arousals during this period of energy conservation. Many studies have been performed to determine why arousal occurs during hibernation, yet it remains poorly understood. A current theory is that rewarming is necessary to repair cellular damage accumulated during torpor (Giroud et al. 2021), which is mediated by restoring cellular processes that have been drastically slowed during torpor (Van Breukelen and Martin 2002; Gillen et al. 2021).

*This paper included in the Focused Collection "Time-Out for Survival: Hibernation and Daily Torpor in Field and Lab Studies" is based on research presented at the 2021 16th International Hibernation Symposium (IHS) organized by Guest Handling Editors Rob Henning, Roelof Hut, and Hjalmar Bouma.

†Corresponding author; email: l.de.wit@rug.nl.

  https://doi.org/10.1086/722904

The T_a's above 4°C decrease torpor bout duration (Pajunen 1983), suggesting that damage accumulation during torpor might be faster at higher T_a's.

Cooling of cells and organs induces DNA damage, which is mediated by reactive oxygen species (ROS) and dependent on both T_a and the duration of cooling (Tolouee et al. 2022). Furthermore, there is controversy over whether antioxidant capacity is harnessed during hibernation. Some studies find that antioxidant capacity is remodeled during hibernation to protect against ROS damage (Drew et al. 2002; Morin and Storey 2007; Dugbartey et al. 2017), while a recent study did not find a difference in antioxidant capacity between summer euthermic and hibernating animals (Duffy and Staples 2022). Despite the various protective mechanisms against cold and ischemia during hibernation, there is increasing evidence for cellular costs due to torpor use. Telomere shortening is a measure for cellular aging and consists of DNA damage to the protective end caps of the DNA. During hibernation, arousal frequency is the best predictor for telomere loss in dormice (Hoelzl et al. 2016; Nowack et al. 2019). Interestingly, lower T_a's during hibernation lead to a faster rate of telomere shortening (Nowack et al. 2019). DNA oxidation damage was not significantly different between torpor, interbout euthermic, and summer euthermic animals; however, lipid damage and protein damage were present, indicating oxidative damage suggested to be ROS mediated (Duffy and Staples 2022). This leads to the questions of whether genomic DNA damage also occurs during hibernation and whether it increases or decreases at lower T_a's. While at very low absolute levels, oxygen consumption in garden dormice during torpor increases by ~40%, with T_a increasing from 4°C to 6°C (Ruf et al. 2021). This increase in oxygen consumption may affect DNA damage levels via ROS accumulation. We therefore hypothesize that faster accumulation of DNA damage occurs at higher T_a's during torpor and is followed by activation of DNA repair pathways. We measured DNA damage in the different torpor groups by alkaline comet assay in splenocytes and by recruitment of the DNA double-strand break (DSB) repair protein 53BP1 by immunohistochemistry in spleen and liver.

Methods

Animals and Experimental Conditions

Before experiments, 39 garden dormice (20 males, 19 females) were moved from group housing (three to five individuals per cage) under natural light/dark and temperature cycles (53°14′33.0″N, 6°32′16.8″E) to a laboratory setting with individual plexiglass cages and an attached wooden nest box (as previously described in Hut et al. 2002*b*) filled with coconut shreds. Ages ranged from 219 to 2,018 d (average = 901.9 ± 650.9 d), and body masses upon entrance into hibernation varied from 96 to 174 g (average = 125.5 ± 19.7 g). Water, sunflower seeds, and chow (Altromin 7024) were given ad lib., although they were rarely consumed during deep hibernation. The animals were kept in complete darkness at T_a's of 5°C, 10°C, or 20°C for at least 6 wk before euthanization. All experimental procedures were performed according to the guidelines of the Animal Welfare Body of the University of Groningen, and all experiments were approved by the Centrale Commissie Dierproeven of the Netherlands (license AVD1050020198666).

Nest Box Temperature and Arousal Detection

Nest box temperature (T_n) was measured continuously using a HOBO Onset pendant (MX2201), which was centrally attached inside the bottom of the nest box, and monitored in real time. Bedding material directly on top of the logger was removed for optimal conductance. Sampling frequency was set at once every 10 min, and the loggers sent out continuous data to a gateway that uploaded the data to the HOBO-Onset web server, allowing for remote access and real-time readout. The T_n data were used to detect the start and end of an arousal through an automated algorithm. In short, data were smoothed by a 200-min running average, allowing detection of an arousal onset when the smoothed T_n increase over 10 min exceeded 10% of the difference between T_n and T_a for three consecutive data points. The end of an arousal was detected when the decrease in T_n over 10 min was between 2.6% and 10% of the difference between T_n and T_a for three consecutive data points. The data were checked manually for false positive or false negative onset and offset detections. Manual inspection of the data showed that this algorithm detected all true arousal onsets and offsets. All false detections, likely caused by movements of the animal, occurred within an arousal and were manually removed.

Temperature Logger Implantations

Subcutaneous intrascapular temperature loggers (Alpha Mach, WeePit, 2.9 g) were used in six animals to measure T_b once every 10 min and to validate the effectiveness of T_n measurements. Implantation procedures were carried out as follows: animals were taken from their home cages, placed in a black anesthesia induction box prefilled with 5% isoflurane, transported to the operation room, and connected to 1%–3% isoflurane with 1 L/min O_2 as the carrier gas for 5–10 min. Fully anesthetized animals were placed on the operation table, where a mouth/nose mask was used to continue the gaseous anesthesia. Throughout the entire anesthesia period, animals were placed on a heating pad, and depth of anesthesia was monitored by observing respiratory rate and the response to pain stimuli to the foot. Body mass was measured, and carprofen (5 mg/kg) was injected subcutaneously to provide analgesic therapy for postsurgical pain (~24 h). Eye ointment was applied to protect against desiccation of the cornea. To avoid dehiscence of the ventral suture by the animal after surgery, we chose a dorsal location. An area (2 cm × 3 cm) caudal of the scapulae was shaved with an electric clipper, leaving ~1 mm of hair length. A midline incision of 1 cm was made, and a subcutaneous pocket was created, allowing implantation of the T_b logger. The skin was closed with the U-suture technique using 5-0 vicryl synthetic and absorbable thread. After surgery, the surgical site was gently cleaned using sterile saline on a swab. Animals were placed back into their recovery cage, and T_b was maintained by a heating pad beneath the cage. Animals were checked daily for welfare issues,

body masses were monitored daily, and animals were placed back into their home cages a week after surgery.

Tissue Collections

Animals were placed into a darkened inhalation box filled with 5% isoflurane and transferred to the operation room. Rectal temperature was measured around 2 min after the animal had been taken from its nest box. After the animal was fully anesthetized, the abdomen was opened, and blood was extracted via a cardiac puncture in the left ventricle, followed by flushing with ~150 mL of saline through the left ventricle. Torpid animals were placed on ice as the animal was flushed with ice-cold saline (0.9% NaCl), and summer euthermic animals were flushed at room temperature. After exsanguination, the brain and internal organs were collected on ice (torpid animals) or at room temperature (summer euthermic animals) and snap frozen at −80°C.

Experimental Groups

The animals were euthanized at different time points during torpor at a T_a of 5°C or 10°C. To determine the different time points, we calculated T_a-specific torpor bout duration (table 1) on the last successful torpor bout for each animal based on nest box logger data. Time points of euthanization were determined by calculating recent torpor bout durations at both T_a's, and they were subsequently established at 1 d in torpor to represent an early torpor group, 4 d in torpor to represent a late torpor group at 10°C, and 8 d in torpor to represent a late torpor group at 5°C. A 4-d torpor group was also included for 5°C for comparison with the 4-d torpor group at 10°C. Summer euthermic animals were investigated in mid-July while they were kept at 20°C and under a 12L : 12D cycle (table 1).

Comet Assay

The comet assay entails electrophoresis of single-cell nuclei embedded in agarose. While intact nuclei remain supercoiled in the head of the comet, fragmented DNA migrates through the gel, creating the comet tail. Alkaline comet assay was performed on freshly isolated splenocytes kept in phosphate-buffered saline (PBS) on ice. Spleen was used to assess DNA damage by comet assay, as single cells may be easily procured by gentle mechanical disruption without the need of digestive enzymes, thereby avoiding artificial DNA damage because of isolation procedures (as is the case, for instance, in liver or small intestines). A positive control was included in all experiments, which consisted of splenocytes treated with a DNA-damaging agent, menadione (27 mg/mL), for 1 h at room temperature.

Spleen was collected, and one-fifth of the tissue was cut into small pieces using a scalpel and suspended in PBS. The cut tissue was gently pushed through a 70-μM cell strainer using the plunger of a 5-mL syringe, collected in PBS, and stored for 1–2 h. Splenocytes were isolated by centrifugation for 3 min at 300 *g*, supernatant was discarded, and pellets were resuspended in PBS to obtain ~0.5×10^6 cells/mL. These procedures were performed on ice and with ice-cold PBS in the case of torpid samples, while procedures and PBS were at room temperature for euthermic samples. Cell suspension aliquots were mixed with 1% low-melting agarose (Trevigen, 4250-050-02) and pipetted on the comet slides (Trevigen, 4250-200-03). Slides were dried for 10 min at 4°C before being submerged in lysis buffer (Trevigen, 4250-010-01) for 2–4 h. Next, slides were treated with unwinding buffer (pH > 13; 200 mM NaOH, 1 mM EDTA) for 30 min in the dark before being subjected to electrophoresis for 30 min at 21 V in alkaline electrophoresis buffer (pH > 13; 200 mM NaOH, 1 mM EDTA) on ice, followed by washing with demineralized water (two times for 5 min) and 70% ethanol (5 min) and by complete drying in an incubator at 37°C for ~30 min. Once dried, the slides were stained with a SYBR gold staining for 30 min, washed with demineralized water three times for 5 min, and left to dry in an incubator for 20 min. Imaging was done using ×10 magnification with fluorescent microscopy.

Fluorescent microscopy images from the comet assay were analyzed using ImageJ. A rectangular box was carefully drawn over the individual nuclei, and fluorescence was measured in the direction of the DNA tails (*y*-axis). Background was measured in each image using the average fluorescence over a box not containing a comet nucleus, and it was subtracted from the plot profile of each nucleus. Data were transformed to cumulative data with total fluorescence for nucleus and tail set to one. The migration distance of the DNA, which increased with the amount of DNA damage and fragmentation, was calculated at the point of 90% and showed how far 90% of the DNA had migrated on the comet slide. A cutoff was calculated based on the average nucleus

Table 1: Experimental groups with time spent in torpor before euthanization in days

Group	Time in torpor (d)	T_a (°C)	Torpor duration (d ± SD)	Range (d)	Comet assay (*N*)	53BPI staining (*N*)	T_n (*N*)	T_b (*N*)
1 d/5°C	1	5	1.6 ± .7	.4–2.6	7	5	7	1
4 d/5°C	4	5	4.4 ± 1.4	1.8–5.7	6	5	6	...
8 d/5°C	8	5	8.2 ± .8	6.9–9.5	6	5	6	1
1 d/10°C	1	10	1.6 ± .7	.4–2.3	7	7	8	1
4 d/10°C	4	10	4.2 ± 1.0	2.7–5.5	8	8	8	3
Euthermia	...	20	...	...	5	4	...	4
Positive control	...	5/10	...	...	8	...	...	...

length of intact and damaged nuclei, plus two times the standard deviation. This cutoff was subtracted from the data to differentiate between intact and damaged nuclei, allowing calculation of the percentage of nuclei showing DNA damage in each sample.

Immunohistochemistry

DSBs were specifically studied by examining DNA DSB repair recruitment (Xie et al. 2007) by 53BP1 staining. Liver tissue and spleen tissue were cut at 4 μm using a cryostat. Tissues were transferred to a Superfrost glass slide (Thermo Fisher Scientific) and dried under a blow-dryer. The slides were then stained for 53BP1 using the following protocol: Dry slides were marked with a Dako pen around the tissue. Slides were fixated in 3% paraformaldehyde for 15 min at room temperature, rinsed for 3 × 5 min in PBS, permeabilized with 0.1% Triton-X in PBS for 10 min, rinsed for 3 × 5 min in PBS, and incubated overnight with primary antibody 53BP1 (H-300, Santa Cruz Biotechnology, sc-22760, rabbit polyclonal IgG) 1:100 in 1% BSA/PBS at 4°C. Then slides were rinsed with PBS and 0.05% Tween (2 × 5 min) to reduce background staining, incubated at room temperature in the dark with Alexa Fluor 488 goat antirabbit IgG 1:500 in 1% BSA for 1 h, rinsed with PBS and 0.05% Tween (2 × 5 min), and rinsed with PBS (2 × 5 min). Next, slides were mounted in Vectashield mounting medium with DAPI to visualize the nuclei. Imaging was done at ×20 and ×100 enlargements, with three images taken per location in red, green, and blue.

Immunohistochemistry images were analyzed using ImageJ, and overlays of the green channel (53BP1 signal) and the blue channel (DAPI, nucleus) were split into separate images. Thresholds were adjusted for each channel to optimize visualization of the signal. Images were made binary, and nuclei were filtered for a median of 10 pixels to ensure processing of viable nuclei. Water shedding was used to separate nuclei that overlap. The analyze particles function of ImageJ calculated the number of nuclei and the 53BP1 signal present in the image. In the overlay of the two channels, the ratio between intracellular and extracellular 53BP1 was determined.

Statistical Analysis

Torpor bout duration and arousal duration at T_a's of 5°C and 10°C were compared using a *t*-test. The percentage of damaged nuclei in the comet assay was arcsine square root transformed to normalize the data distribution. The amount of 53BP1 foci per nucleus was log transformed to normalize for skewing toward zero. The effects of T_a, days in torpor, and their interactions on DNA damage and repair (53BP1 staining) were determined by using a one-way ANOVA with a least significant difference all-pairwise comparisons test. Correlation between comet damage and 53BP1 repair recruitment was calculated on transformed data by using a Pearson's test. Sex, body mass, and age effects on comet damage were calculated using linear models. Statistical significance was determined at $P < 0.05$. All statistical analyses were performed using R (ver. 4.0.2.) with the R package agricolae, and figures were generated using the R package ggplot2.

Results

Nest Box Temperature and Body Temperature in Garden Dormice

The T_n data accurately overlapped with the T_b data for timing of arousals (fig. 1). No arousals were missed while using T_n-based arousal detection, and T_n was further used to determine the onset and offset of all arousals. Animals kept at $T_a = 10$°C

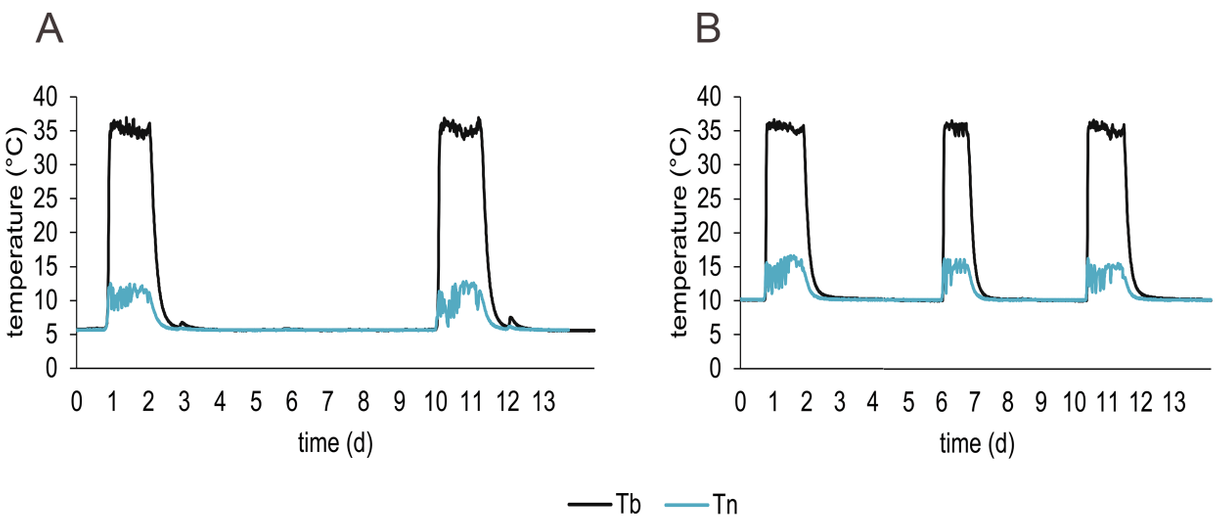

Figure 1. Relationship between nest box temperature (T_n) and body temperature (T_b) at different ambient temperatures (T_a's). Graphs depict both T_b and T_n in degrees Celsius, illustrating that T_n accurately indicates timing of arousals in the torpor-arousal cycle. *A*, T_b and T_n measured at a constant T_a of 5°C. *B*, Higher T_a (10°C) shortens torpor bout duration.

showed a ~22% reduction of torpor bout duration compared to animals kept at 5°C (5°C = 8.20 ± 3.10 d, 10°C = 6.58 ± 2.58 d, $P < 0.05$), while arousal duration did not differ significantly between groups (5°C = 1.04 ± 0.58 d, 10°C = 1.42 ± 0.60 d).

DNA Damage in Splenocytes

The percentage of nuclei showing DNA damage at T_a = 5°C increased significantly between the first day of torpor and the middle of the torpor bout (4 d), but it did not increase further between 4 and 8 d (figs. 2*B*, 2*C*, 3*A*). In contrast, at T_a = 10°C, a high amount of damaged nuclei was already found at day 1 of torpor compared to summer euthermia, without the further increase in percentage of DNA-damaged cells found at 4 d in torpor. Thus, torpor at 10°C for 1 d seemed to generate more damaged nuclei compared to torpor at 5°C, yet this trend was not statistically significant ($P = 0.081$). At 4 d of torpor, no difference in splenocyte DNA damage was observed between animals kept at 5°C or 10°C. Linear models showed significant

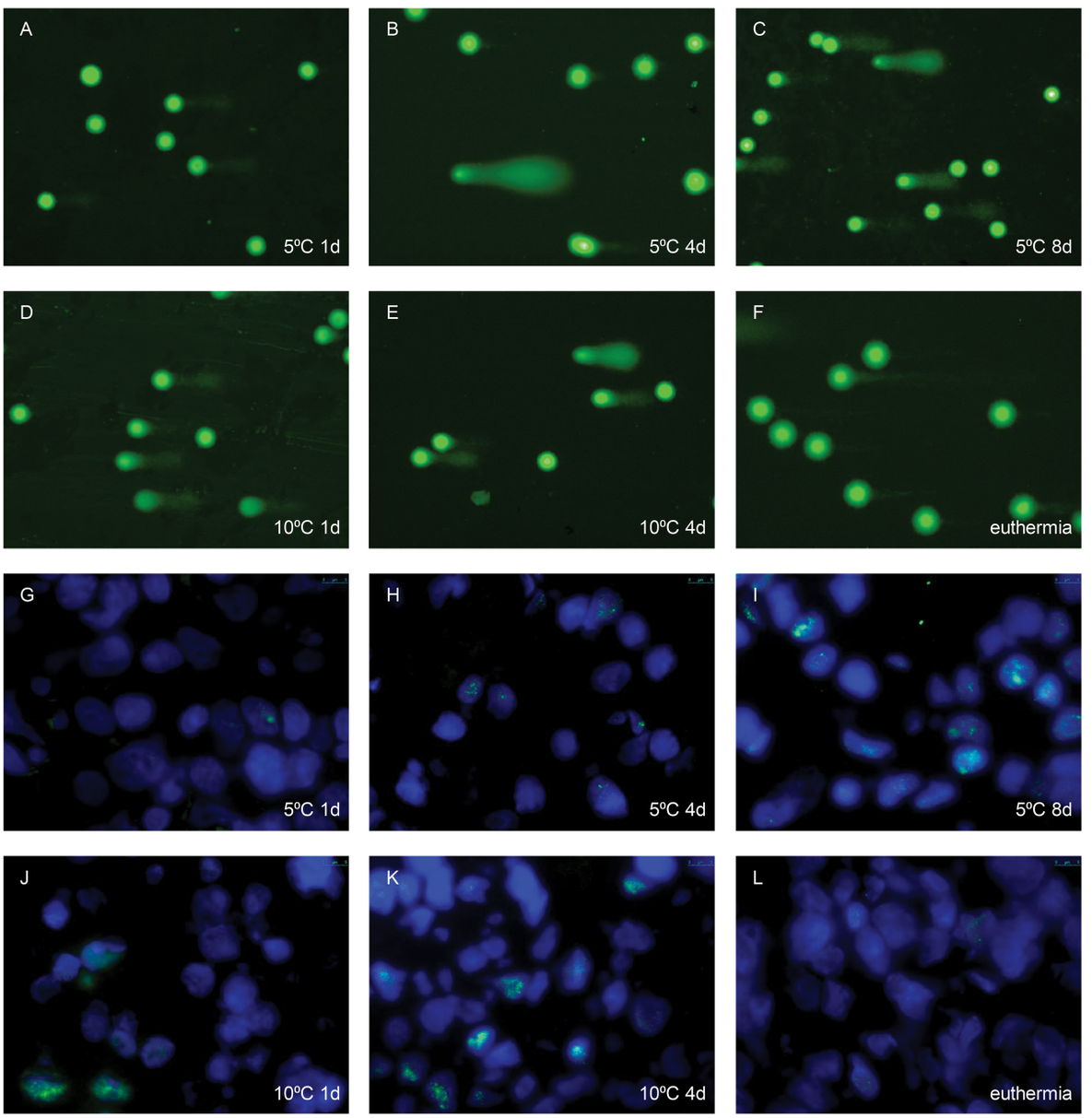

Figure 2. Microscopy images of DNA damage and repair in spleen at 5°C and 10°C. *A–F*, Single-cell gel electrophoresis (comet assay) measuring DNA damage. Intact DNA remains supercoiled in the nucleus, and tails indicate fragmented DNA pulled from the nucleus. *G–L*, Immunohistochemistry for 53BP1 foci (green) involved in the DNA damage response for double-strand breaks in the nucleus (DAPI, blue).

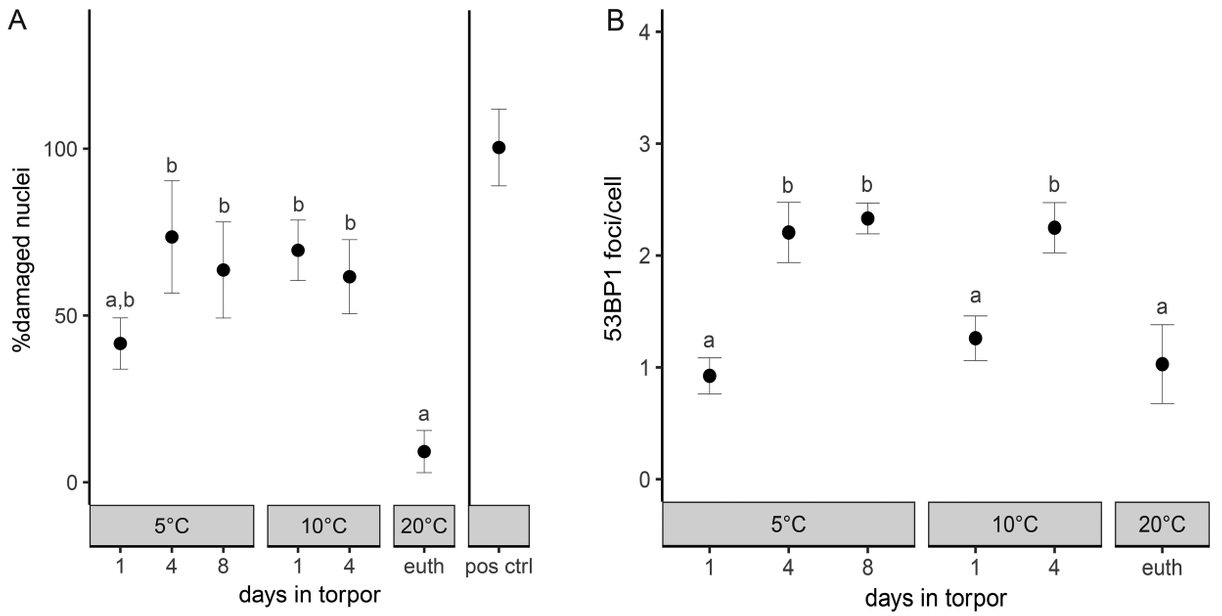

Figure 3. DNA damage and repair in spleen at 5°C and 10°C. *A*, Percentage of splenocyte nuclei that show a damaged tail in the alkaline comet assay. Average error and standard error are plotted for the experimental groups based on ambient temperature and days spent in torpor. All torpor groups, except for 1 d in torpor at 5°C, differ significantly from the summer euthermic group. *B*, Average number of 53BP1 foci per nucleus with standard error. Summer euthermia and 1 d in torpor at 5°C and 10°C differ significantly from 4 and 8 d in torpor at 5°C and 10°C. Euth = euthermia; pos ctrl = positive control.

correlations of damaged nuclei with sex ($R^2 = 0.299$, $P = 0.015$), with males showing overall less damaged splenocytes compared to females (fig. A1), and a significant negative correlation of damaged nuclei with body mass ($R^2 = 0.121, P = 0.018$). Age did not correlate significantly with damaged nuclei ($R^2 = 0.0054$, $P = 0.2803$).

Mounting of DNA Double-Strand Break Repair

Immunohistochemistry was performed on liver tissue and spleen tissue to quantify the recruitment of the DNA DSB repair protein 53BP1 by counting the number of foci per nucleus (fig. 3*B*). In this way, we specifically addressed the number of DSBs, which are intrinsically more prone to faulty repair. The number of 53BP1 foci at day 1 of torpor was similar to summer euthermia, both in animals kept at 5°C and in animals kept at 10°C. Likewise, both 5°C and 10°C animals showed an increase in 53BP1 foci at day 4 in torpor, which persisted until day 8 in the 5°C group. In liver, a similar pattern of increased 53BP1 foci at day 4 of torpor was found, yet 8 d of torpor at 5°C caused a significant further increase in the number of 53BP1 foci compared to 4 d (fig. A2). 53BP1 recruitment in spleen and liver did not depend on age ($P > 0.1$).

Correlation between DNA Damage and Repair in Spleen

To explore the dynamics between DNA damage and repair during hibernation, we correlated data of comet assay with spleen 53BP1, showing a significant positive correlation ($R^2 = 0.774, P = 0.001$; fig. A3). Low T_a (5°C) showed a low amount of damaged nuclei after 1 d in torpor and subsequently a low amount of repair recruitment reflected in a low number of 53BP1 foci. At 4 d, an increase in DNA damage was observed in some animals that also showed high 53BP1 levels. At 8 d of torpor at 5°C, DNA damage and the number of 53BP1 foci stayed similar to those at 4 d of torpor, indicating a strong positive correlation between damage and repair recruitment at 5°C (fig. 4). At 10°C, high levels of DNA damage were observed after 1 d of torpor, but the repair pathway by 53BP1 was not recruited yet. After 4 d, 53BP1 was recruited, and DNA damage levels stayed at a similar level as at day 1. Collectively, this resulted in a nonsignificant correlation between damage and repair recruitment at 10°C (fig. 4). Spleen damage and liver repair recruitment were correlated ($R^2 = 0.636$, $P = 0.017$; fig. A5), and this suggested a similar impact of torpor on liver DNA damage and repair.

Discussion

In hibernating garden dormice, we showed differences in DNA damage levels and recruitment of DNA repair pathways by 53BP1 during torpor in spleen tissue. Higher T_a decreases torpor bout duration and increases DNA damage before the first 4 d in torpor. DNA damage accumulates over the first 4 d in torpor at 5°C and in the first 24 h in torpor at 10°C. DNA repair recruitment at 5°C is activated at 4 d in torpor, when DNA damage is accumulated, and stays active at 8 d in torpor. At 10°C, the recruitment of repair factors is lagging with low levels of 53BP1 at 1 d in torpor, while

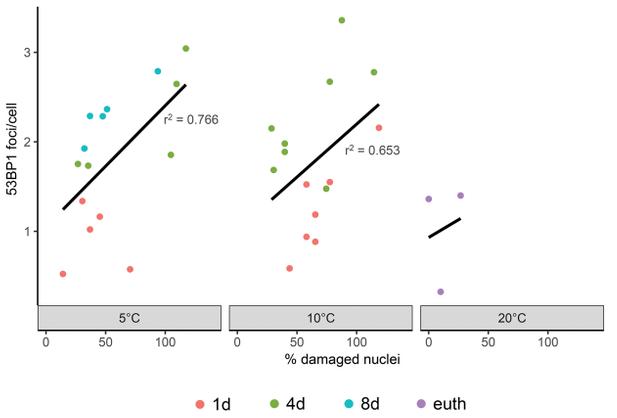

Figure 4. Correlation between DNA damage in comet assay and double-strand break repair in 53BP1 staining in spleen tissue. In the three panels, a linear regression is plotted between the percentage of damaged nuclei and the number of 53BP1 foci for the animals kept at 5°C ($P = 0.021$), 10°C ($P = 0.112$), and 20°C. Red represents 1 d in torpor, green represents 4 d in torpor, blue represents 8 d in torpor, and purple represents euthermia.

DNA damage levels are already high, and with an increase of repair recruitment at 4 d in torpor. The latter results in a mismatch at 10°C with a faster accumulation of DNA damage yet a slow recruitment of DNA repair pathways.

DNA Damage during Torpor

During euthermia, T_b's of deep hibernators are maintained between 36.5°C and 38°C, which likely optimizes the balance of enzymatic processes in the body. In torpor, T_b also remains strictly regulated around 0°C even when T_a drops below 0°C. Above a T_a of 0°C , torpor T_b closely follows T_a and remains ~1.5°C above ambient. This results in a much broader T_b range during torpor, possibly resulting in a suboptimal balance in enzymatic function. This large range in torpor T_b may lead to mitochondrial dysfunction and increased production of ROS (Trachootham et al. 2008). Hibernators are prepared to deal with the ischemic conditions during torpor—much better prepared than nonhibernators—by increasing antioxidant capacity (Drew et al. 2002; Morin and Storey 2007), using tissue remodeling (Talaei et al. 2012), and suppressing mitochondrial respiration (Brown et al. 2012). Despite these adaptive mechanisms, there are higher levels of ROS damage, as shown by increased lipid peroxidation, during hibernation than during summer euthermia (B. M. Duffy, unpublished manuscript). Such an increase in ROS levels during hibernation may well constitute the source of the observed DNA damage. In turn, DNA damage can also lead to an increase in intracellular ROS as a stress response (Rowe et al. 2008). ROS are known to induce different types of DNA damage, such as lipid peroxidation, deoxyribose damage (Rowe et al. 2008), and DNA base modifications, all of which are measured by the alkaline comet assay (Collins 2004). The alkaline comet assay measures different types of DNA damage, such as DSBs and single-strand breaks, because of its unwinding step. The alkaline treatment converts alkali-labile sites to breaks (Singh et al. 1988; Azqueta et al. 2014). Consequently, the total number of DNA strand breaks measured by alkaline comet assay exceeds the number of DSBs, which were more specifically investigated using 53BP1 staining.

Unexpectedly, we found strong sex differences in DNA damage during torpor, where females seemed to accumulate considerably more damage, as indicated by splenocyte comet assays (fig. A1). The difference in damage is normalized during euthermia, and the cause of these sex differences needs to be further elucidated.

Possible Consequences of DNA Damage during Torpor

Cell mitosis is paused during torpor, but it is highly active during arousals, suggesting a repair mechanism during the arousal periods (Vinogradova 1988; Popov et al. 2011). Temporary quiescence through cell cycle arrest during torpor (Wu and Storey 2012) can allow for time to repair the DNA damage accumulated during hibernation. Apoptosis seems to be actively blocked during hibernation (Logan et al. 2016; Logan and Storey 2017), indicating that complete renewal of DNA-damaged cells is unlikely. Activation of these processes may serve to enable deployment of the DNA damage response and repair of accumulated DNA damage, which seems to be the prevailing strategy of deep hibernators.

Surveillance and Repair of DNA Damage during Torpor

During torpor, the accumulating DNA damage is sensed, and subsequently DNA repair mechanisms are recruited, as evident by the increase in recruitment of the DNA DSB repair protein 53BP1. 53BP1 is translocated to the nucleus at 4 d in torpor in both the 5°C and 10°C groups and likely marks sites containing DSBs for repair.

Temperature affects protein function, as evidenced most prominently in the slowing of enzymatic activity during cooling (Malan 2010). However, our data indicate that DNA damage surveillance and recruitment of subsequent repair mechanisms may be upregulated during torpor. The recruitment of DNA repair mechanisms could be deemed effective, as there is no further increase of DNA damage beyond 4 d of torpor at 5°C as well as no further increase of DNA damage at 10°C after 1 d of torpor is observed.

In conclusion, this study documents an increase in genomic DNA damage during torpor compared to summer euthermia. DNA damage and repair recruitment dynamics differ with T_a in torpid garden dormice, suggesting a temperature-dependent fast accumulation of DNA damage at the start of a torpor bout, probably because of lagging DNA repair recruitment. The observed DNA damage during hibernation is in contrast with the longer life expectancy in hibernators (Lyman et al. 1981; Turbill et al. 2011), suggesting effective or even overcompensating DNA repair during hibernation.

Acknowledgments

We thank the animal caretakers of the University of Groningen, notably Diane ten Have, for their help with the garden dormouse colony.

Literature Cited

Azqueta A., J. Slyskova, S.A.S. Langie, I. O'Neill Gaivao, and A. Collins. 2014. Comet assay to measure DNA repair: approach and applications. Front Genet 5:288.

Brown J.C.L., D.J. Chung, K.R. Belgrave, and J.F. Staples. 2012. Mitochondrial metabolic suppression and reactive oxygen species production in liver and skeletal muscle of hibernating thirteen-lined ground squirrels. Am J Physiol 302: R15–R28.

Buck C.L. and B.M. Barnes. 2000. Effects of ambient temperature on metabolic rate, respiratory quotient, and torpor in an arctic hibernator. Am J Physiol 279:R255–R262.

Collins A.R. 2004. The comet assay for DNA damage and repair: principles, applications, and limitations. Mol Biotechnol 26: 249–261.

Drew K.L., O. Tøien, P.M. Rivera, M.A. Smith, G. Perry, and M.E. Rice. 2002. Role of the antioxidant ascorbate in hibernation and warming from hibernation. Comp Biochem Physiol C 133:483–492.

Duffy B.M. and J.F. Staples. 2022. Arousal from torpor increases oxidative damage in the hibernating thirteen-lined ground squirrel (*Ictidomys tridecemlineatus*). Physiol Biochem Zool 95:229–238.

Dugbartey G.J., M.C. Hardenberg, W.F. Kok, H.V. Carey, J.F. Staples, R.H. Henning, and H.R. Bouma. 2017. Renal mitochondrial response to low temperature in non-hibernating and hibernating species. Antioxid Redox Signal 27:599–617.

Geiser F. and G.J. Kenagy. 2016. Torpor duration in relation to temperature and metabolism in hibernating ground squirrels. Physiol Zool 61:442–449.

Gillen A.E., R. Fu, K.A. Riemondy, J. Jager, B. Fang, M.A. Lazar, and S.L. Martin. 2021. Liver transcriptome dynamics during hibernation are shaped by a shifting balance between transcription and RNA stability. Front Physiol 12:662132.

Giroud S., C. Habold, R.F. Nespolo, C. Mejías, J. Terrien, S.M. Logan, R.H. Henning, and K.B. Storey. 2021. The torpid state: recent advances in metabolic adaptations and protective mechanisms. Front Physiol 11:623665.

Hoelzl F., J.S. Cornils, S. Smith, Y. Moodley, and T. Ruf. 2016. Telomere dynamics in free-living edible dormice (*Glis glis*): the impact of hibernation and food supply. J Exp Biol 219: 2469–2474.

Hut R.A., B.M. Barnes, and S. Daan. 2002*a*. Body temperature patterns before, during, and after semi-natural hibernation in the European ground squirrel. J Comp Physiol B 172:47–58.

Hut R.A., E.A. Van der Zee, K. Jansen, M.P. Gerkema, and S. Daan. 2002*b*. Gradual reappearance of post-hibernation circadian rhythmicity correlates with numbers of vasopressin-containing neurons in the suprachiasmatic nuclei of European ground squirrels. J Comp Physiol B 172:59–70.

Logan S.M., B.E. Luu, and K.B. Storey. 2016. Turn down genes for WAT? activation of anti-apoptosis pathways protects white adipose tissue in metabolically depressed thirteen-lined ground squirrels. Mol Cell Biochem 416:47–62.

Logan S.M. and K.B. Storey. 2017. Avoiding apoptosis during mammalian hibernation. Temperature 4:15–17.

Lyman C.P. 1948. The oxygen consumption and temperature regulation of hibernating hamsters. J Exp Zool 6:204–220.

Lyman C.P., R.C. O'Brien, G.C. Greene, and E.D. Papafrangos. 1981. Hibernation and longevity in the Turkish hamster *Mesocricetus brandti*. Science 212:668–670.

Malan A. 2010. Is the torpor-arousal cycle of hibernation controlled by a non-temperature-compensated circadian clock? J Biol Rhythms 25:166–175.

Morin P.J. and K.B. Storey. 2007. Antioxidant defense in hibernation: cloning and expression of peroxiredoxins from hibernating ground squirrels, *Spermophilus tridecemlineatus*. Arch Biochem Biophys 461:59–65.

Nowack J., I. Tarmann, F. Hoelzl, S. Smith, S. Giroud, and T. Ruf. 2019. Always a price to pay: hibernation at low temperatures comes with a trade-off between energy savings and telomere damage. Biol Lett 15:20190466.

Pajunen I. 1983. Ambient temperature dependence of the body temperature and of the duration of the hibernation periods in the garden dormouse, *Eliomys quercinus* L. Cryobiology 20:690–697.

———. 1992. A comparison of the heart rate at different ambient temperatures during long-term hibernation in the garden dormouse, *Eliomys quercinus* L. Cryobiology 29:414–421.

Popov V.I., I.V. Kraev, D.A. Ignat'ev, and M.G. Stewart. 2011. Suspension of mitotic activity in dentate gyrus of the hibernating ground squirrel. Neural Plast 2011:867 525.

Rowe L.A., N. Degtyareva, and P.W. Doetsch. 2008. DNA damage-induced reactive oxygen species (ROS) stress response in *Saccharomyces cerevisiae*. Free Radic Biol Med 23:1–7.

Ruf T., K. Gasch, G. Stalder, H. Gerritsmann, and S. Giroud. 2021. An hourglass mechanism controls torpor bout length in hibernating garden dormice. J Exp Biol 224:jeb243456.

Singh N.P., M.T. McCoy, R.R. Tice, and E.L. Schneider. 1988. A simple technique for quantitation of low levels of DNA damage in individual cells. Exp Cell Res 175:184–191.

Talaei F., H.R. Bouma, M.N. Hylkema, A.M. Strijkstra, A.S. Boerema, M. Schmidt, and R.H. Henning. 2012. The role of endogenous H2S formation in reversible remodeling of lung tissue during hibernation in the Syrian hamster. J Exp Biol 215:2912–2919.

Tolouee M., K.D.W. Hendriks, F.F. Lie, L.P. Gartzke, M. Goris, F. Hoogstra-Berends, S. Bergink, and R.H. Henning. 2022. Cooling of cells and organs confers extensive DNA

strand breaks through oxidative stress and ATP depletion. Cell Transplant 31:09636897221108705.

Trachootham D., W. Lu, M.A. Ogasawara, N.R. Del Valle, and P. Huang. 2008. Redox regulation of cell survival. Antioxid Redox Signal 10:1343–1374.

Turbill C., C. Bieber, and T. Ruf. 2011. Hibernation is associated with increased survival and the evolution of slow life histories among mammals. Proc R Soc B 278:3355–63.

Van Breukelen F. and S.L. Martin. 2002. Reversible depression of transcription during hibernation. J Comp Physiol B 172:355–361.

Vinogradova M.S. 1988. Mitotic activity of stomach epithelium in the ground squirrel, *Citellus erythrogenys* brandt. Comp Biochem Physiol A 91:235–239.

Wu C.W. and K.B. Storey. 2012. Pattern of cellular quiescence over the hibernation cycle in liver of thirteen-lined ground squirrels. Cell Cycle 11:1714–1726.

Xie A., A. Hartlerode, M. Stucki, S. Odate, N. Puget, A. Kwok, G. Nagaraju, et al. 2007. Distinct roles of chromatin-associated proteins MDC1 and 53BP1 in mammalian double-strand break repair. Mol Cell 28:1045–1057.